

### Effects of Monomer Shape on the Formation of Fractal Aggregates Under a Power Law Distribution

Jonathan D. Perry, Jesse Kimery, Lorin S. Matthews and Truell W. Hyde, Center for Astrophysics, Space Physics and Engineering Research (CASPER), Baylor University, One Bear Place 97310, Waco, Texas 76798-7310, USA ([Jonathan.Perry@baylor.edu](mailto:Jonathan.Perry@baylor.edu), [Lorin.Matthews@baylor.edu](mailto:Lorin.Matthews@baylor.edu), [Truell.Hyde@baylor.edu](mailto:Truell.Hyde@baylor.edu))

**Introduction:** Dusty plasmas occur in a variety of environments, such as the interstellar medium (ISM), protoplanetary disks (PPDs), Earth's atmosphere, and industrial processes. It is therefore important to understand how particles interact with each other and how their structures may differ based upon the physical characteristics of the particles themselves or their environment. A detailed study of the microphysics that governs the evolution of aggregate structures is a key component to accurately modeling the evolution of the dust population.

A number of computer models have been developed to explore the behavior of interacting and colliding dust grains under various conditions [1-4]. A near ubiquitous assumption in these models has been spherical monomers as the building blocks of larger aggregate structures. Deviation from the simple spherical structure is motivated by evidence via the polarization of sunlight from cometary dust which suggests the presence of non-spherical dust particles, specifically with a major axis three times longer than the minor axes [6]. Recent work has shown that using shapes which deviate from spherical symmetry may produce aggregates with significantly differing morphologies, altering the coagulation behavior [5].

A previous study examined coagulation of ellipsoidal particles using a monodisperse population undergoing low-velocity ballistic collisions [5]. This work modeled prolate ellipsoids with an axis ratio of 3:1:1 and compared the resulting structures to those grown using spherical monomers. This study will expand upon the previous work in two ways: 1) additional axis ratios will be explored, including oblate ellipsoids in addition to prolate ellipsoids and 2) populations of polydisperse monomers will be modeled to accurately reflect size distributions in astrophysical environments.

**Methods:** In this study, the creation of aggregates occurs by simulating pair-wise interactions of particles. The model employed has previously been used to examine the coagulation of charged particles, the coagulation considering the influence of magnetic materials, as well as the coagulation of ellipsoidal monomers [3, 4, 5, 7]. The model employs a large parameter space for monomers which affect low-velocity collisions such as radius, impact parameter, rotations, charge, density, magnetization and dipole interactions. The model was modified to allow user-specified axis ratios as well as exponential size distributions

characterized by  $n(r) dr = r^{-\alpha} dr$ , where  $r$  is the semi-major axis (or radius) of a monomer and  $\alpha$  is an exponent typically ranging from  $\alpha = 1.8 - 3.5$  for astrophysical environments [8].

Maximum and minimum radii used in each model varied depending on the shape. The prolate ellipsoidal monomers have a semi-major axis ranging from  $r = 0.25 \mu\text{m} - 5 \mu\text{m}$ , with an axis ratio of 3:1:1. The radii for the spherical and oblate ellipsoidal monomers were chosen so the smallest and largest monomers would have equivalent volumes in all cases. Oblate ellipsoidal monomers used an axis ratio of 3:3:1.

Aggregates, which consist of an increasing number of monomers, originate as a single monomer which is placed at the origin of a coordinate system. A new monomer is generated at a random position a distance  $20R$  away from the initial particle, where  $R$  is the maximum radius of a monomer or aggregate measured from the center of mass (COM) of the aggregate. Particles are also given a random initial orientation, important for non-spherical particles. Initial velocities are set according to Brownian motion with the temperature set to 100 K, for illustrative purposes. The particles are assumed to be silicates with a density of  $\rho = 2.51 \text{ g/cm}^3$ . Particle trajectories are directed towards the COM of the initial particle with an offset ranging from 0 to  $1/2(R_1 + R_2)$ , half the sum of the radii of the two particles. As the incoming particle approaches within a distance  $(R_1 + R_2)$ , the closest two monomers in each particle are examined to determine when overlap occurs. In the low-velocity regime employed here, the particles are assumed to stick at the point of contact and be held together via Van der Waals forces without the possibility of rolling or sliding.

Aggregates are grown using a combination of particle-cluster aggregation (PCA) and cluster-cluster aggregation (CCA) collisions. First generation aggregates ( $N \leq 20$ ) are grown through PCA collisions, adding a single monomer to each aggregate each collision. After a collision, the new particle's attributes (mass, spin, etc.) are calculated and stored for analysis and future use to create larger aggregates. Second and third generation aggregates, ( $20 < N \leq 200$ ) and ( $200 < N \leq 2000$ ) respectively, are grown through CCA collisions, with incoming clusters being drawn from the previous generation(s).

**Results:** The influence of monomer shape is determined by comparing the morphology of the

resulting aggregates, here characterized by the compactness factor.

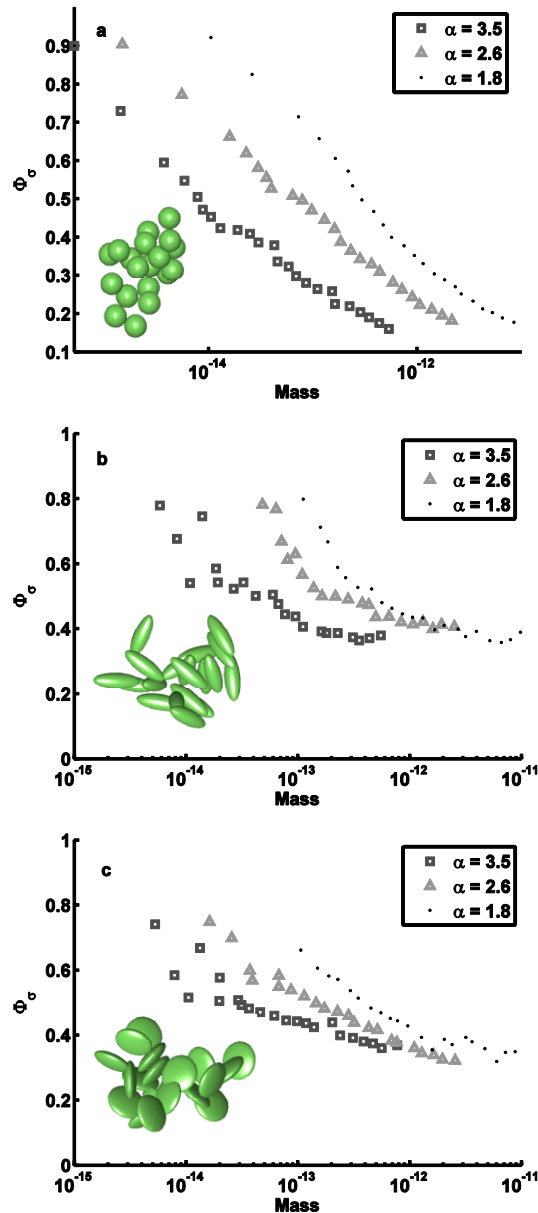


Figure 1. Compactness factors versus mass for a) spherical monomers, b) prolate ellipsoidal monomers and c) oblate ellipsoidal monomers. A representative aggregate from the monodisperse population is also shown for each monomer shape.

The compactness factor is a measure of how fluffy and open or compact an aggregate structure is. Lower compactness factors correspond to more open structures, while high compactness factors correspond to more compact or spherical aggregates. The compactness factor is calculated by

$$\phi_\sigma = \frac{\sum r_i^3}{R_\sigma^3}$$

where  $r_i$  corresponds to the radius of the individual monomers for spheres, while for ellipsoidal shapes  $r_i$  is defined as the average radius of the monomer, and  $R_\sigma$  is the radius of the average projected cross-section of the aggregate.

Compactness factors for the various populations of aggregates grown in this study are shown in Figure 1. Aggregates constructed from spheres (Figure 1a) exhibit similar trends for all values of  $\alpha$ , growing to more open structures as monomers are added approaching compactness factors of less than 0.2, which are very fluffy. Prolate ellipsoidal monomers (Figure 1b) exhibit a similar trend to the spherical monomers, but tend to a higher compactness factor of approximately 0.4. Oblate ellipsoidal monomers (Figure 1c) tend to a compactness factor of approximately 0.3 as they grow to large size, intermediate to the previous two cases. From Figures 1b and 1c it may be seen that aggregates composed of ellipsoidal monomers tend to be more compact (less fluffy) than aggregates composed of spheres. For any given mass, independent of monomer shape, populations which have a greater  $\alpha$  tend to be fluffier.

By combining the differences exhibited by the compactness factors with additional physical parameters, such as cross-sectional area, which affects collision probability, and friction time, which affects the relative velocities, a determination may be made as to whether the shape of dust monomers has a non-negligible effect. These parameters may be utilized in a statistical study of the evolutions of a dust population in PPDs via the Smoluchowski equation. The underlying microphysics are incorporated in this equation via the coagulation kernel, which depends on the collision cross-section, relative velocities and sticking efficiency of the particles, all of which are directly related to the compactness factor.

**References:** [1] Dominik, C., H. Nubold (2002) *Icarus*, 157 [2] Ormel, C. W., M. Spaans, A.G.G.M. Tielens, (2006) *A&A* [3] Matthews, L. S., T. W. Hyde (2004) *IEEE Trans. On Plasma Sci.*, 32 [4] Perry, J., L. S. Matthews, T. W. Hyde, (2010) *IEEE Trans. On Plasma Sci.*, 38 [5] Perry, J., E. Gostomski, L. S. Matthews, T. W. Hyde, (2012) *A&A*, accepted for publication [6] Hage, H. I, J. M. Greenberg, (1990), *Astroph. Journal*, 361 [7] Matthews, L. S., T. W. Hyde, (2008), *IEEE Trans. On Plasma Sci.*, 36 #1 [8] Ossenkopf, V, (1993), *A&A*, 280.